

Multiple magnetic flux entry into superconducting quantum-interference devices (SQUIDS): A general way of examining the $\cos\phi$ conductance

Robert L. Peterson

Electromagnetic Technology Division, National Bureau of Standards, Boulder, Colorado 80303

Robert I. Gayley

Department of Physics, State University of New York at Buffalo, Amherst, New York 14260

(Received 13 February 1978)

A new type of experiment is proposed for obtaining information about the $\cos\phi$ conductance of the Josephson effect. Based on measurement of fluxoid entry into a superconducting ring broken by a Josephson junction, the technique is to operate in the low-damping regime for which the voltage excursions associated with fluxoid entry are small. For this case, the constant-voltage expression containing the $\cos\phi$ conductance should be valid. It is shown that the erraticity associated with the low-damping regime has a predictable statistical pattern, which is rather insensitive to noise but quite sensitive to the $\cos\phi$ term. A shunt resistance can be used to vary the average voltage. Statistics can be accumulated over a large number of similar loops, or over one or a few loops at slightly varying bath temperature between runs, or even over one loop at one temperature provided the noise at the junction has appropriate properties. Thus, the technique would appear to be capable of estimating the controversial coefficient of the $\cos\phi$ term as a function of voltage and temperature for any type of junction for which low damping can be achieved.

I. INTRODUCTION

The observation of multiple magnetic fluxoid entry, or "quantum transitions," into superconducting quantum-interference devices (SQUIDS)—superconducting rings which are broken by Josephson junctions—has been reported in many articles, usually with a qualitative or semiquantitative discussion of the underlying reasons for the multiple fluxoid entry (see, e.g., Ref. 1). In a typical experiment, a magnetic field is applied in a direction normal to the plane of the ring. When the applied flux reaches a certain threshold value, many magnetic flux quanta will enter through the junction in rapid succession. No more fluxoids enter the ring until the external flux reaches a second threshold, whereupon another group enters, etc.

Some recent articles²⁻⁵ have reported results of detailed simulations of this phenomenon, using simple models for the junction. Smith and Blackburn² have shown that for rings with "high" damping β and large values of $\gamma \equiv LI_c/\Phi_0$ (symbols are defined later), the number of flux quanta entering the loop as the external magnetic flux reaches threshold is a unique and predictable function of the SQUID parameters. However, at small damping the number entering was shown by Wang and Gayley³ to become erratic (or more accurately, extremely sensitive to small changes in parameters). The latter authors⁴ later inserted the $\cos\phi$ conductance^{6,7} into their simulations and showed that it can greatly affect the number of fluxoids entering the loop in the high-damping region. The measurement of the number of fluxoids entering

the ring thus could give useful information about the $\cos\phi$ conductance, a question which is now very much unsettled.⁷⁻¹⁵ However, Gayley and Wang⁴ cautioned that the high rapidly varying voltages expected to develop during the flux entry might render invalid the starting point of the calculation, namely the constant-voltage assumption^{6,7} which leads to the appearance of an explicit $\cos\phi$ term. That this is probably true is shown later in the present paper, as well as possibly by a recent high-damping experiment⁵ in which the measured flux entry did not agree at all with simulations, with or without the $\cos\phi$ term (see also Ref. 2 in this regard).

In this paper we consider especially the "erratic" low-damping case in more detail, for several reasons. First, erratic behavior is commonly observed in loops¹⁶⁻²⁰ and elsewhere.^{21,22} Second, as we show later, the significant voltage change occurs over a time interval much longer than the inherent response times (picoseconds) of superconducting materials, thus, validating the constant-voltage expression [Eq. (1)] in the computations. And, finally, it is evident that the $\cos\phi$ term should have a marked influence on flux entry in the low-damping regime as well as at high damping.

In the absence of noise and for a particular choice of parameter values and initial conditions, there is of course, one value for the final flux in the loop. However, at low damping, a small change in parameter values or a pulse of noise can result in a large change in the final flux. In this paper we argue that in spite of this, meaningful measurements can in fact be made with such a system. For

a reasonable amount of noise and a reasonable range of parameter values, the final flux will be distributed in a predictable way over a small subset of values. Therefore, the statistical distribution of a series of trials can be predicted. Since the $\cos\phi$ term affects this distribution, the experiment should yield a value for the coefficient of this term. Further, since the maximum voltage developed is controllable by a shunt resistance, such an experiment offers the possibility of determining the $\cos\phi$ coefficient as a function of voltage, a type of experiment not yet attempted. Tunnel junctions are here implied, because the damping constant can readily be made small with them. However, the theory and technique presented here would apply to any type of junction for which low damping could be achieved.

Finally, in the Appendix, we show by a simple argument the source of an empirical formula deduced from the simulations,² relating the damping to γ for single fluxoid admission. We also present a more accurate simple expression valid to within 1% down to $\gamma \approx 1$. Knowledge of this relationship is important because some Josephson devices based on flux counting could give misleading results if more than one fluxoid enters at a time.

II. BASICS

The circuit analyzed is that of the simple junction shunted by capacitance and a phase-dependent conductance, and connected to a superconducting loop of inductance L (see Fig. 1). The tunnel current $I(t)$ into the junction, indicated in Fig. 1, was first derived by Josephson⁶ for a tunnel junction to be

$$I(t) = I_c \sin\phi + \sigma_0 V + \sigma_1 V \cos\phi, \quad (1)$$

in which a constant voltage V across the junction was assumed. The coefficients I_c , $\sigma_0 \equiv 1/R$, and σ_1 are voltage dependent. The ratio σ_1/σ_0 has been calculated by Poulsen¹³ at several temperatures, from tunneling theory, and is indicated schemati-

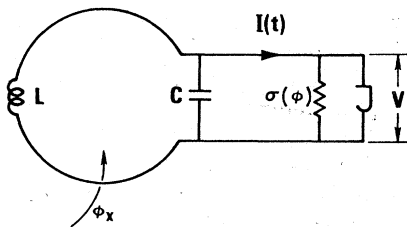


FIG. 1. Circuit used in the simulations of this paper. The three elements on the right comprise the Josephson junction. The tunnel current $I(t)$, as shown after the capacitance, is given in Eq. (1).

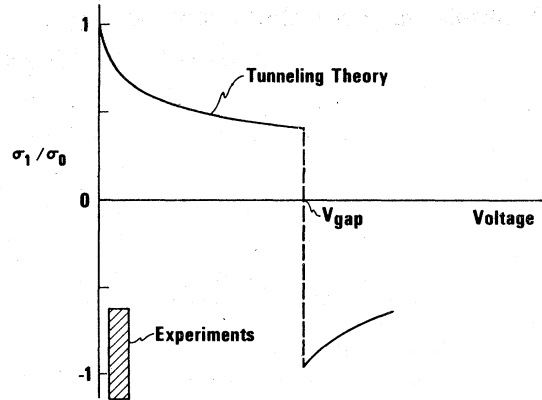


FIG. 2. Schematic diagram illustrating the dependence of σ_1/σ_0 upon voltage (solid curve), according to tunneling theory. The shaded rectangle indicates the locations of experimental determinations of σ_1/σ_0 for tunnel, microbridge, and point contact junctions. A recent experiment (Ref. 15) carried out on tunnel junctions at several temperatures near the critical temperature, showing both signs for σ_1/σ_0 , but opposite to that expected from tunneling theory, is not shown.

cally in Fig. 2. The rectangle in Fig. 2 also indicates, with one recent exception,¹⁵ the results of experiments designed to measure σ_1/σ_0 , for tunnel, microbridge, and point-contact junctions. The vertical dimension of the rectangle is meant to suggest the error bars associated with most of the experiments. As is seen, the experiments tend to agree with each other. The results have a sign opposite to that predicted from tunneling theory, but are in approximate agreement with Landau-Ginsburg theory.^{7,12} A recently published experiment¹⁵ on tunnel junctions at temperatures very close to the critical temperature shows, however, a sign change as a function of temperature.

When an external magnetic field is applied to the loop of Fig. 1, the differential equation describing the circuit becomes

$$\frac{d^2\phi}{dt_1^2} + \beta \frac{d\phi}{dt_1} \left(1 + \frac{\sigma_1}{\sigma_0} \cos\phi \right) + 2\pi\gamma \sin\phi + \phi = \phi_x, \quad (2)$$

where $t_1 = t/\sqrt{LC}$, $\beta = \sqrt{LC}/RC$, $\gamma = LI_c/\Phi_0$, I_c is the junction critical current (here assumed unaffected by the magnetic field which would typically be $\lesssim 10^{-6}\text{T} = 10^{-2}\text{G}$), ϕ is the superconducting phase difference across the junction, ϕ_x is the applied magnetic flux in units of $\Phi_0/2\pi$, and $\Phi_0 = 2.068 \times 10^{-15}\text{Vs}$ is the flux quantum. I_c , σ_0 , and σ_1 are taken to be constants in our simulations. The resistance R is the quasiparticle tunneling resistance combined with any shunt resistance that may be present. In an experiment the resistance will be taken from the dc current-voltage characteristic

of the junction. In our calculations, we suppose that some average R is used, but it would be a simple matter to use the measured voltage-dependent resistance if this seemed desirable. The average voltage may be appreciably less than the gap voltage, so the tunneling resistance may be much larger than the normal state resistance of the junction. A shunt resistor may be inserted to obtain the desired value of β or to adjust the value of the average voltage.

Most of the remaining discussion in this section repeats material published earlier.^{2,3} We feel it desirable to include it, however, because of the important insights provided by the potential-well picture. Note that the present ϕ and ϕ_x are equal to the earlier^{2,3} Φ and Φ_x multiplied by 2π .

When ϕ_x is changing adiabatically, Eq. (2) can be cast into the intuitively appealing form

$$\frac{d}{dt_1}(\mathcal{T} + \mathcal{V}) = -\beta \left(1 + \frac{\sigma_1}{\sigma_0} \cos \phi\right) \left(\frac{d\phi}{dt_1}\right)^2, \quad (3)$$

where the "kinetic energy" \mathcal{T} is $\frac{1}{2}(d\phi/dt_1)^2$, and the "potential energy" \mathcal{V} is

$$\mathcal{V} = \frac{1}{2}(\phi - \phi_x) - 2\pi\gamma \cos \phi. \quad (4)$$

The term on the right-hand side of Eq. (3) represents viscous drag modulated by the $\cos \phi$ term.

The state of the system may be visualized as a particle moving along the potential \mathcal{V} (see Fig. 3). As the field is raised slowly from zero, the particle stays at the bottom of the local well near $\phi = 0$ until ϕ_x is large enough that the local minimum is now an inflection point (and also the local maximum), whereafter the particle begins to "slide" until stopped by the damping.

The extrema of \mathcal{V} are given by

$$\frac{\partial \mathcal{V}}{\partial \phi} = 0 = \phi + 2\pi\gamma \sin \phi - \phi_x, \quad (5)$$

and the inflection points by

$$\frac{\partial^2 \mathcal{V}}{\partial \phi^2} = 0 = 1 + 2\pi\gamma \cos \phi. \quad (6)$$

The solution of Eq. (6) for ϕ , substituted into Eq.

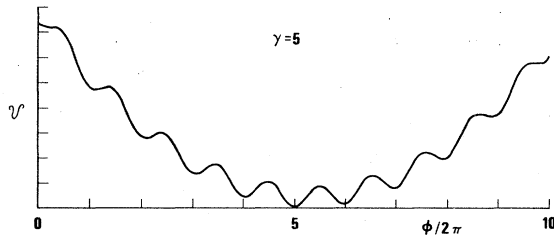


FIG. 3. "Potential" \mathcal{V} of Eq. (4) plotted for $\gamma = 5$ and $\phi_x = 5.253 \times 2\pi$.

(5), specifies what ϕ_x must be at the beginning of the motion of the particle. One finds for the "break-in" value of the externally applied normalized flux

$$\begin{aligned} \phi_x &= \cos^{-1} \left(-\frac{1}{2\pi\gamma} \right) + \left(4\pi^2\gamma^2 - 1 \right)^{1/2} \\ &= 2\pi\gamma + \frac{\pi}{2} + \frac{1}{4\pi\gamma} + O(\gamma^{-2}), \end{aligned} \quad (7)$$

and for the starting inflection point ϕ_i ,

$$\phi_i = \cos^{-1}(-1/2\pi\gamma) = \frac{3}{2}\pi + 1/2\pi\gamma + O(\gamma^{-2}). \quad (8)$$

The next inflection point at positive slope is of course at $2\pi + \phi_i$. Its adjacent minimum and maximum are at $\frac{5}{2}\pi \pm (2/\gamma)^{1/2} + O(\gamma^{-1})$. The intermediate inflection point is at $2\pi - \phi_i = \frac{3}{2}\pi - \frac{1}{2}\pi\gamma + O(\gamma^{-2})$. The latter quantities will be used in the Appendix, where we consider threshold damping for single fluxoid admission.

Figure 3 shows a plot of the potential \mathcal{V} , Eq. (4), for $\gamma = 5$, and ϕ_x equal to its "break-in" value of $2\pi \times 5.253$. Note that there are about γ local wells between the starting inflection point and the bottom of the "bowl," or overall potential. Thus, if the particle stops at the bottom, γ fluxoids have been admitted into the loop. We shall use the terminology "high damping" and "low damping" to mean, respectively, the cases in which the particle stops before reaching the bottom, or sweeps past it.

III. BEHAVIOR AT LOW DAMPING, WITHOUT NOISE

As mentioned earlier, when Gayley and Wang⁴ introduced the $\cos \phi$ term into their simulations at high damping and found a large effect, they cautioned that large voltage excursions might be expected which would possibly invalidate their starting point, Eq. (1). That this is true is shown in Fig. 4 for $\gamma = 100$ and $\beta = 12$, a typical high-damp-

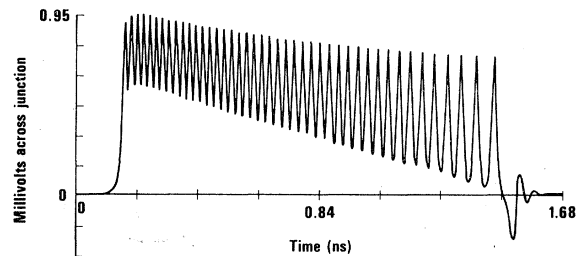


FIG. 4. Typical high-damping case: $\beta = 12$, $\gamma = 100$. Circuit parameters which give these values of β and γ are, for example, $L = 2000$ pH, $C = 14$ pF, $I_c = 0.1$ mA, $R = 1$ Ω , $\sigma_1 = 0$. The time and voltage scales are based on these values. The gap voltage is not determined by the RI_c product, since R is not necessarily the junction normal-state resistance.

ing case. The voltage excursions approach 100% of the maximum voltage developed. Note that there is an infinitude of ways of choosing L , C , R , and I_c for given γ and β . For the values indicated in the caption, each voltage excursion takes place in about 30 ps. After fluxoid entry begins, some 43 fluxoids enter the loop in about 1 ns. Figure 4 can also be thought of as particle velocity as a function of time. The particle is trapped 0.43 of the way to the bottom of the bowl, whereupon it undergoes damped oscillations (the plasma oscillations) about the bottom of the local well.

The low-damping regime, however, is quite different. Here the voltage excursions are typically very small, and only the voltage envelope is important. Figure 5 illustrates a moderate damping case, with $\gamma = 484$ and $\beta = 1.77$. Even on a greatly expanded scale (not shown) the voltage excursions are scarcely discernible until the particle is nearly trapped, and even then the amplitudes are very small. For the typical circuit parameters used in Fig. 5, the voltage envelope, corresponding to the entry of about 480 fluxoids, develops over a time of about 3 ns, much longer than the picosecond response times of typical superconducting materials. The junction will thus readily follow this adiabatically varying voltage, and Eq. (1) should be a valid basis for simulations. An accurate calculation would incorporate the voltage dependence of σ_1/σ_0 , but since this is "unknown"—this is what the experiment is all about—we treat it as a constant; the experiment then would determine σ_1/σ_0 as a function of the average voltage developed during flux entry. By means of a shunt resistance, the latter can be varied from values comparable to the gap voltage to much smaller values. In Fig. 5, for example, suppose that the gap voltage is 2 mV. Then the resistance of 2 Ω implies use of a shunt resistance only slightly greater than 2 Ω , since with $I_c = 0.4$ mA the normal junction resistance would be about 8 Ω .

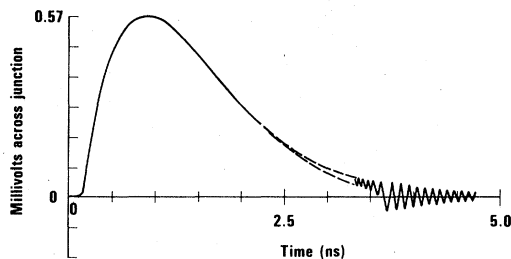


FIG. 5. Moderately low-damping case: $\beta = 1.77$, $\gamma = 484$. Circuit parameters, which determine the time and voltage scales, are: $L = 2500$ pH, $C = 200$ pF, $I_c = 0.4$ mA, $R = 2$ Ω , $\sigma_1 = 0$. The dashed lines indicate the voltage extrema.

The resistance on the low-voltage portion of the I - V curve actually being sampled would be considerably greater. As is seen, the average voltage developed during the flux entry is about 0.2 mV, or 10% of the assumed gap voltage.

A complicating effect occurs in the low-damping regime, however. Wang and Gayley³ showed that the final state of the system seems to be erratic. Actually, the final state is a very sensitive but predictable function of the system parameters. An example is shown in Fig. 6 for $\beta = 1.20$, $\sigma_1 = \sigma_0$, and γ in the neighborhood of 1000. Here, there are two preferred final states, one near a final flux number of 1100 (the particle sweeps past the bottom of the bowl and is trapped about 10% up on the opposite wall), and the other near 1000 (the particle does not get trapped on the opposite wall, but falls back to near the bottom). These fluxoid numbers are consistent with the "approximate theoretical maximum and minimum" computed from Eq. (1) of Wang and Gayley.³ Guéret²³ has also found two final states in a related calculation. For yet lower values of damping, there can be more than two possible final states.

For a damping constant near 1.2 and γ near 1000, the final fluxoid number for $\sigma_1 = +\sigma_0$ in, for example, the upper state differs by only a few from the upper state number for $\sigma_1 = -\sigma_0$. Thus, counting of fluxoids would have to be accurate within about 1% in this example, in order to determine a value for σ_1/σ_0 with error bars less than ± 1 . Although this may be possible, there is a much more important reason why fluxoid counting from a single measurement would be inadequate for examining the $\cos\phi$ term in low-damping loops. As we see from Fig. 6, it is not likely that we could know the γ of a given loop to sufficient precision to predict whether the final fluxoid number would be, for example, 1000 or 1100. Even if we knew γ accurately,

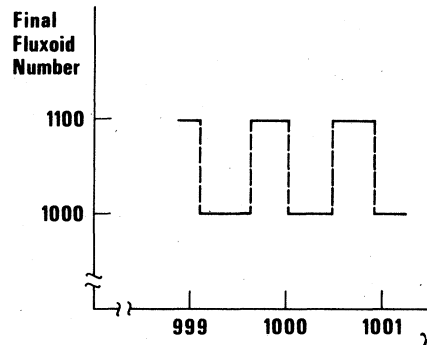


FIG. 6. Final flux values in a superconducting loop with damping constant of 1.20, $\sigma_1 = \sigma_0$, and γ near 1000. Two states are selected by the system in an almost periodic fashion.

ly on one run, its value on a subsequent run would be slightly different if the bath temperature changed slightly. Thus, what would be obtained on a series of runs would be a statistical distribution over the possible final states.

We have observed that the "occupation numbers" of the final states are quite sensitive to the $\cos\phi$ term, yet insensitive to noise. That is, the fraction of the cases in which the system will end in a given preferred final state is sensitive to the value of σ_1/σ_0 , and this fraction is readily determined from the simulations by varying γ in small increments. Thus, instead of having to count fluxoids with great precision, one has the attractive alternative of accumulating statistics, using relatively crude fluxoid counting. In such a procedure, one could fabricate a series of superconducting rings with closely similar values of γ . The individual values would presumably be distributed somewhat randomly within a small range, and the results of the flux measurements would be a statistical distribution of values among the preferred final states.

Rather than making measurements on a large number of similar loops, one would probably prefer to make repeated measurements on one or a few loops, deliberately varying the bath temperature slightly between measurements, for example, a few millidegrees. Since γ is proportional to I_c , which in turn is proportional to the temperature-dependent energy gap, this procedure would seem to be a convenient method for varying γ in small steps. Still another procedure (here anticipating the results of Sec. IV) might be to make repeated measurements on one or a few junctions at a "fixed" temperature, allowing the noise at the junction to be the statistical generator. As we shall see in Sec. IV, the noise parameters would have to fall in a certain range.

Table I shows the results of a ratio analysis at $\beta = 1.18, 1.20, \text{ and } 1.22$, which is a reasonable range of uncertainty for this parameter. The Table entries show the percentage of the total number of possible times that the flux entry will be found in the upper of the two final states; they are determined by incrementing γ in very small steps, and are accurate to ± 0.1 (for the noise-free entries). The difference of more than a factor of 2 between the results at $\sigma_1/\sigma_0 = +1$ and -1 should make the distinction between these values readily discernible. The ultimate accuracy of the determination of σ_1/σ_0 will depend principally upon the amount of statistics accumulated. The effects of noise are discussed in Sec. IV.

There are of course other values of β and γ which may be appropriate. We selected the range displayed in Table I because just two well-separated

TABLE I. The entries in the σ_1 columns are the percentage of occurrences for which the final flux entry into the superconducting loop is in the high-flux state (about 1100 in this case). Values of γ near 1000 are used, with damping values β as shown. The last row indicates the results of noise simulations at a noise frequency of $1000/\sqrt{LC}$ and a noise amplitude of $0.1\phi_x$. Some 228 simulations using different sets of (pseudo) random numbers are used for each value of σ_1 in the noise simulations. The uncertainties indicated correspond to one standard deviation (Ref. 25).

β	$\sigma_1 = +\sigma_0$	$\sigma_1 = 0$	$\sigma_1 = -\sigma_0$	Noise amplitude
1.18	37.8	27.7	16.5	0
1.20	40.6	30.0	18.1	0
1.22	43.6	32.4	19.8	0
1.20	43 ± 3.3	29 ± 3.0	17 ± 2.5	$0.1\phi_x$

final states occur. Lower damping might result in, for example, three final states, two of which would likely be fairly close to each other, and possibly confuse the results. However, this is not necessarily so, because one might simply examine the well-separated state, unless its percentage occupancy is so low that adequate accumulation of statistics becomes difficult.

IV. EFFECTS OF NOISE

It is important to understand the effects of noise on the results of Sec. III. Noise may be pictured as a rocking of the "bowl," representing the potential energy \mathcal{V} , about its bottom. That is, from Eq. (4), the variation of the potential due to a variation $\delta\phi_x$ in ϕ_x is

$$\delta\mathcal{V} = (\phi_x - \phi)\delta\phi_x. \quad (9)$$

Thus, one might anticipate that noise would tend to make the flux entry more regular—the particle tends to get shaken toward the bottom of the bowl. For a particle trapped high on the wall of the bowl, which can occur only for very low damping, noise can fairly easily displace the particle from its relatively shallow local well. But for moderately low damping, in which the particle is trapped, for example, 10% above the bottom of the bowl, noise of "ordinary" amplitude will not displace the particle once the particle has settled down, which occurs after several plasma oscillation periods. One should also note that in addition to tending to prevent trapping in a certain well, noise can also promote trapping in a well in which the particle would not remain in the noise-free case. There is a strong symmetry in these two cases, which our simulations bear out.

Noise enters primarily through ϕ_x —even Johnson noise in the junction or shunt resistance²⁴ can be

lumped into ϕ_x . A "second-order" effect would lie in the variations of γ because of variations in I_c , e.g., because ϕ_x is noisy, but this can surely be ignored. Thermal fluctuations could also affect I_c through the energy gap, but both the amplitude and frequency would be too low to be of significance for temperatures not too close to T_c .

We have examined the effects of noise by adding to ϕ_x a suitably distributed (pseudo)random number at each new time increment in the computation (or at some multiple thereof, thereby varying the noise frequency, or spectrum). Noise levels (standard deviations) up to 10% of ϕ_x have been used.

It is evident that the "erraticity" at low damping will be dependent upon noise frequency. If the particle has not had time to settle to the bottom of a local well, a pulse of noise has a fair probability of kicking the particle out. Thus, the natural frequency against which to compare noise frequency is the plasma frequency, which is the frequency of the motion of the particle in a local well. This is readily obtained from Eq. (2) by setting $\phi = 2\pi n + \phi'$ where $|\phi'| \ll 1$ and n is an integer. The homogeneous solution to the equation thus linearized (and here dropping the "cos ϕ term") is $\exp(\rho t_1)$ where

$$\rho = -\frac{1}{2}\beta \pm [\beta^2 - 4(1 + 2\pi\gamma)]^{1/2}. \quad (10)$$

Since β^2 is less than about 9γ for multiple flux entry (see the Appendix), this is an underdamped case. Further, if $\beta^2 \ll 8\pi\gamma$, which is the ordinary case for low damping, the angular plasma frequency ω_p is just $(8\pi\gamma)^{1/2}$ in t_1 space, or $(8\pi\gamma/LC)^{1/2}$ in real time. The damping time is $2/\beta \approx \frac{1}{2}\gamma^{1/2}$, the inequality being the condition for multiple transitions, as above. Thus, the damping time is greater than the plasma period $2/(8\gamma/\pi)^{1/2}$, and the particle will always make several swings through the bottom of a local well before coming to rest.

The plasma period has a significance beyond that of a trapped particle: a particle traveling slowly, but not quite slowly enough to be trapped, clearly will require about one-half the plasma period in traveling from one local maximum to the next. Thus, we can easily estimate the time required, or the number of noise pulses occurring, when the particle moves from a fluxoid number of, for example, 1100 to 1000, to use the example of Sec. III.

There are two effects of noise which must be considered. (i) By how much does noise produce scatter about the preferred final states, and are the mean values shifted from the noise-free case? (ii) By how much does noise affect the ratios of the "occupation numbers" in the (now spread-out) final states? We anticipate that the preferred experimental procedure would be that of determining

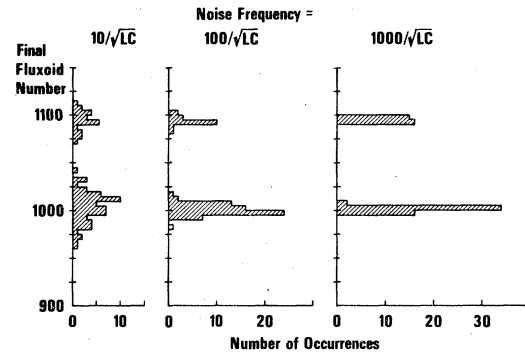


FIG. 7. Histograms showing how different noise frequencies affect the final flux values in a superconducting loop. Noise amplitude = $0.05\phi_x$; $\beta = 1.20$; $\sigma_1 = 0$; nine values of γ in the range from 999.0 to 1001.7. About 80 runs were made at each noise frequency.

the ratios. Thus, question (i) is not important unless the scatter is so great that the clusters overlap.

That the mean values of the final states should not be materially affected by noise, as seen in Fig. 7, is intuitive: The preferred states are determined by the values of β and γ . If, for example, a small change of γ changes the trapping point from the upper to the lower of two preferred states, by the same reasoning a noise kick on the trapped particle near the extreme of its plasma oscillation swing can eject the particle and cause it to seek the lower preferred state.

Scattering obviously increases with increasing noise amplitude. The example of Fig. 7 shows no overlap between clusters even at the relatively large noise amplitude of $0.05\phi_x$. The influence of noise frequency upon the scatter is, however, not so easy to understand, and certainly not easy to explain in a few words. Since the question is not important in the present context, we shall offer only the following: When the noise frequency is low, the last noise pulse before trapping (or nontrapping) is important and may cause trapping in an "abnormal" state, thus, causing scatter. When the noise frequency is high, however, there is a great amount of self-cancellation of the noise, and the scatter is smaller. Our simulations do show that for noise frequencies ω_N less than ω_p , there is a good bit of scatter about the final states, whereas for $\omega_N \gg \omega_p$, the clustering is quite narrow. Figure 7 illustrates this for three values of noise frequency: $10/\sqrt{LC}$, $100/\sqrt{LC}$, and $1000/\sqrt{LC}$. These are to be compared to the plasma frequency $\sqrt{2\gamma/\pi}/\sqrt{LC} \approx 25\sqrt{LC}$ for $\gamma \approx 1000$.

The important question is number (ii) above. One expects that the occupation number ratios will not be greatly affected by "reasonable" noise

amplitudes since the trapping and nontrapping situations should be affected rather symmetrically by the noise. All the simulations we have made bear this out. Table I illustrates this for γ near 1000 and β near 1.2, at the very large noise amplitude of $0.1 \phi_x$ and a noise frequency of $1000/\sqrt{LC}$. The 228 calculations made for each value of σ_1 result in an uncertainty in the listed percentages as shown by the indicated standard deviations.²⁵ Calculations at smaller noise amplitudes have also been made, and also show the insensitivity of the percentages to noise.

Finally, our simulations with noise show that the percentages are not biased by choice of γ , for a given β . For example, if we consider only those values of γ , within the range 999–1001, for which the final state would be the lower of the two possible states in the noise-free case, we find the same percentages as given in Table I to within our statistical significance. Thus, an experiment making repeated runs on a single junction, allowing the noise at the junction to generate the statistics, may be an acceptable technique. Of course, the noise amplitude has to be large enough to be effective, but not so large as to produce chaotic results. Our simulations have shown that quite a broad range of noise amplitude is acceptable. A noise frequency comparable to or larger than the plasma frequency would also be desirable.

V. CONCLUSIONS

We conclude that it should be possible to derive useful information about the $\cos\phi$ conductance by measurement of fluxoid entry into a superconducting loop at low damping. Low damping ensures that the basic equation containing the $\cos\phi$ term is a valid basis for this type of experiment.

The procedure described in this paper should greatly improve our knowledge of σ_1 at low voltage. Moreover, by use of a shunt resistance, the average voltage developed during flux entry can be controlled, and thus σ_1/σ_0 can be estimated as a function of voltage, a dependence which has not been measured to date. Since tunneling theory predicts a large discontinuity in σ_1/σ_0 at the gap voltage, with a sign reversal, measurements near such voltage would be particularly exciting.

The temperature dependence of σ_1/σ_0 could also be obtained, obviously, by varying the bath temperature. It would be interesting to compare such results with those recently obtained.¹⁵

Noise is not likely to be an obscuring factor, according to our calculations and may be desirable in accumulating statistics.

Finally, provided low damping can be achieved, the experiment can be performed with any type of Josephson junction. This could be very interesting because to date each type of junction—tunnel, microbridge, or point contact—has used an entirely different experimental method for examining the $\cos\phi$ conductance.

Measurement of fluxoid entry at *high* damping can also be made, but as Gayley and Wang⁴ pointed out, a theory allowing for a dynamic voltage²⁶ should then be used to calculate the expected fluxoid number. Since the theory for large rapidly varying voltage would not have an explicit $\cos\phi$ term, one could not then speak of determining the value of σ_1/σ_0 , but only of confirming or denying the validity of the complete theory.

ACKNOWLEDGMENTS

We wish to thank our colleagues in the cryoelectronics group of the Natl. Bur. Stand. (U. S.) for many invigorating discussions. Part of this work was done while one of us (R. I. G.) was a guest worker at Natl. Bur. Stand. (U. S.). He wishes to thank the staff for its hospitality. This work was supported in part by the Office of Naval Research Contract No. N0001477C0415.

APPENDIX

In this Appendix we consider the threshold damping for single fluxoid entry, in order to show the source of a relation deduced empirically from earlier simulations.^{2,5} We also develop a more accurate expression valid over a larger range of γ .

To examine the threshold damping in question, we ask: What must be the value β_1 of the damping constant β in order that the particle not slide beyond the first maximum of the potential \mathcal{U} at $\frac{5}{2}\pi + (2/\gamma)^{1/2}$? (The positions of the first few extrema and inflection points of \mathcal{U} were obtained in Sec. II.) The relation deduced empirically^{2,5} for γ in the region above 100 is $\beta_1 = 3.0\gamma^{1/2}$. To show the source of this relation we use the following simple argument. First, we observe that for $\gamma \gg 1$, as illustrated in Fig. 8 for $\gamma = 200$, the potential energy curve is quite steplike initially, rather than having pronounced minima and maxima. This suggests approximating the potential by the piecewise linear portions shown in Fig. 8. We draw a horizontal line through ϕ_{\max} , and a straight line with the correct negative slope of $-4\pi\gamma$ through the inflection point near $\phi = \frac{3}{2}\pi$. One can easily show,

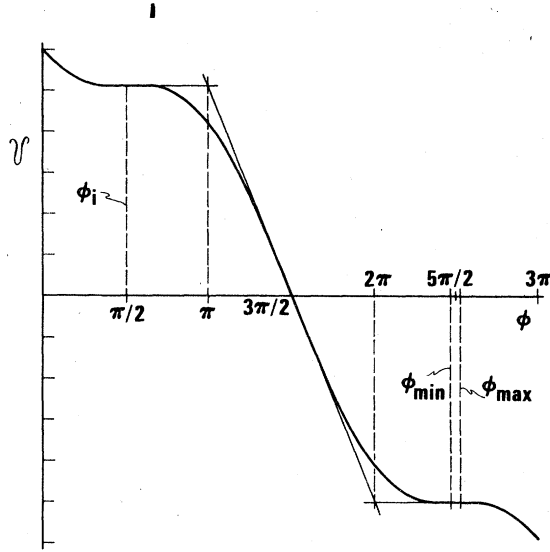


FIG. 8. First portion of the potential \mathcal{U} for $\gamma=200$ and $\phi_x=2\pi \times 200,250$, together with the piecewise linear portions used to approximate \mathcal{U} in this region. The vertical scale is arbitrary.

once β_1 is estimated, that the particle sliding down the linear slope will nearly have its terminal velocity

$$\left. \frac{d\phi}{dt_1} \right|_{\text{terminal}} = \frac{4\pi\gamma}{\beta}, \quad (\text{A1})$$

when the horizontal portion is reached. On a horizontal line, the particle travels a distance equal to its initial velocity divided by the damping constant; that is,

$$\phi_{\text{stop}} = \phi_{\text{start}} + \frac{1}{\beta} \left. \frac{d\phi}{dt_1} \right|_{\text{terminal}}. \quad (\text{A2})$$

Setting the asymptote ϕ_{stop} equal to $\frac{5}{2}\pi$, and ϕ_{start} equal to 2π [the intersection of the two straight lines is at $2\pi + O(\gamma^{-1})$], requires $\beta_1 = (2/\pi) \times (d\phi/dt_1)|_{\text{terminal}}$, which with Eq. (A1) gives

$$\beta_1 = (8\gamma)^{1/2}, \quad (\text{A3})$$

which has the observed square-root behavior. Note that $8^{1/2} = 2.83$. Note also that if in Eq. (A2) the asymptote is refined to $\frac{5}{2}\pi + (2/\gamma)^{1/2}$ then Eq. (A3) becomes

$$\beta_1 = (8\gamma)^{1/2} - 4/\pi; \quad (\text{A4})$$

that is, an offset is predicted. We have made a computer study of β_1 vs γ down to values for which β_1 vanishes. The expression

$$\beta_1 = 2.99\gamma^{1/2} - 2.53, \quad (\text{A5})$$

is accurate to within 1% for all values of γ above unity. For $\gamma < 1$, β_1 dips slightly below this line and falls to zero at $\gamma_{\text{min}} = 0.733$. At this value, the second maximum of \mathcal{U} has risen to the level of the starting point, so that even at zero damping, not more than one fluxoid can enter the loop. γ_{min} is the solution of

$$2\pi\gamma \cos(4\pi^2\gamma^2 - 1)^{1/2} = -1, \quad (\text{A6})$$

which results from requiring that $\phi + 2\pi\gamma \sin\phi$ have the same value at ϕ_i as at $4\pi - \phi_i$.

Knowledge of threshold damping is important because any Josephson device acting as a flux counter in some measurement process could give quite misleading results if more than one fluxoid would enter at a time. For example, in the analog-to-digital conversion of a continuous signal which causes fluxoid entry or expulsion from a superconducting loop, the reconstructed signal could be quite distorted if this occurred.²⁷

¹D. B. Sullivan, R. L. Peterson, V. E. Kose, and J. E. Zimmerman, *J. Appl. Phys.* **41**, 4865 (1970).

²H. J. T. Smith and J. A. Blackburn, *Phys. Rev. B* **12**, 940 (1975).

³T. C. Wang and R. I. Gayley, *Phys. Rev. B* **15**, 3401 (1977).

⁴R. I. Gayley and T. C. Wang, *Phys. Rev. B* **16**, 3270 (1977).

⁵J. A. Blackburn, H. J. T. Smith, and V. Keith, *Phys. Rev. B* **15**, 4211 (1977).

⁶B. D. Josephson, *Phys. Lett.* **1**, 251 (1962); *Rev. Mod. Phys.* **36**, 210 (1964); *Adv. Phys.* **14**, 419 (1965).

⁷H. Højgaard Jensen and P. E. Lindelof, *J. Low Temp. Phys.* **23**, 469 (1976).

⁸D. N. Langenberg, *Rev. Phys. Appl.* **9**, 35 (1974).

⁹N. F. Pedersen, R. F. Finnegan, and D. N. Langenberg, *Phys. Rev. B* **6**, 4151 (1972).

¹⁰C. M. Falco, W. H. Parker, and S. E. Trullinger, *Phys. Rev. Lett.* **31**, 933 (1973).

¹¹M. Nisenoff and S. Wolf, *Phys. Rev. B* **12**, 1712 (1975).

¹²D. A. Vincent and B. S. Deaver, Jr., *Phys. Rev. Lett.* **32**, 212 (1974); R. Rifkin, D. A. Vincent, and B. S.

Deaver, Jr., *J. Appl. Phys.* **47**, 2645 (1976); B. S. Deaver, Jr., R. Rifkin, and R. D. Sandell, *J. Low Temp. Phys.* **25**, 409 (1976).

¹³U. K. Poulsen, *Rev. Phys. Appl.* **9**, 41 (1974).

¹⁴R. E. Harris, *Phys. Rev. B* **10**, 84 (1974).

¹⁵O. H. Soerensen, J. Mygind, and N. F. Pedersen, *Phys. Rev. Lett.* **39**, 1018 (1977).

¹⁶A. M. Goldman, P. J. Kriesman, and D. J. Scalapino, *Phys. Rev. Lett.* **15**, 495 (1965).

¹⁷R. C. Jaklevic, J. Lambe, J. E. Mercereau, and A. H. Silver, *Phys. Rev.* **140**, A1628 (1965).

¹⁸J. Wilson and R. I. Gayley, *Solid State Commun.* **11**, 1183 (1972).

¹⁹T. A. Fulton, L. N. Dunkleberger, and R. C. Dynes, *Phys. Rev. B* **6**, 855 (1972).

²⁰N. H. Zappe and K. R. Grebe, *J. Appl. Phys.* **44**, 865

(1973).

²¹T. A. Fulton and R. C. Dynes, *Solid State Commun.* **9**, 1069 (1971).

²²T. A. Fulton, *Appl. Phys. Lett.* **19**, 311 (1971).

²³P. Guéret, *J. Appl. Phys.* **44**, 1771 (1973).

²⁴R. L. Peterson and D. G. McDonald, *IEEE Trans. Mag.* **MAG-13**, 887 (1977).

²⁵The noise entries ($m \pm s$) are made as follows: the number of times the system ends in the high state, divided by the number of trials (228), and multiplied

by 100, gives the main entry m . The percentage standard deviation s is determined by adopting the sample mean ($m/100$) as true mean, computing the standard deviation of each trial about this mean, multiplying by $\sqrt{228}$ to determine the sample standard deviation, and finally multiplying by $100/228$ to obtain s .

²⁶N. R. Werthamer, *Phys. Rev.* **147**, 255 (1966).

²⁷R. L. Peterson and D. B. Sullivan (unpublished).